THE JOURNAL OF BIOLOGICAL CHEMISTRY VOL. 289, NO. 42, pp. 28971–28986, October 17, 2014

Interleukin-17 (IL-17)-induced MicroRNA 873 (miR-873) Contributes to the Pathogenesis of Experimental Autoimmune Encephalomyelitis by Targeting A20 Ubiquitin-editing Enzyme*[S]

Received for publication, April 28, 2014, and in revised form, August 19, 2014 Published, JBC Papers in Press, September 2, 2014, DOI 10.1074/jbc.M114.577429

Xiaomei Liu, Fengxia He, Rongrong Pang, Dan Zhao, Wen Qiu, Kai Shan, Jing Zhang, Yanlai Lu, Yan Li, and Yingwei Wang[1]

From the Department of Microbiology and Immunology, Nanjing Medical University, Hanzhong Road 140, Nanjing, Jiangsu 210029, China

Background: The regulatory mechanism of abnormal miRNA expression in astrocytes upon IL-17 stimulation remains unclear.
Results: miR-873 induced by IL-17 promotes inflammatory cytokine production and aggravates demyelination in experimental autoimmune encephalomyelitis (EAE) through the A20/NF-κB pathway.
Conclusion: IL-17 regulates miRNA expression in astrocytes, which affects the pathogenesis of EAE.
Significance: These data provide a novel regulatory mechanism in inflammatory autoimmunity diseases.

Interleukin 17 (IL-17), produced mainly by T helper 17 (Th17) cells, is increasingly recognized as a key regulator in various autoimmune diseases, including human multiple sclerosis (MS) and its animal model, experimental autoimmune encephalomyelitis (EAE). Although several microRNAs (miRNAs) with aberrant expression have been shown to contribute to the pathogenesis of MS and EAE, the mechanisms underlying the regulation of abnormal miRNA expression in astrocytes upon IL-17 stimulation remain unclear. In the present study, we detected the changes of miRNA expression profiles both in the brain tissue of EAE mice and in cultured mouse primary astrocytes stimulated with IL-17 and identified miR-873 as one of the co-up-regulated miRNAs *in vivo* and *in vitro*. The overexpression of miR-873, demonstrated by targeting A20 (TNFα-induced protein 3, TNFAIP3), remarkably reduced the A20 level and promoted NF-κB activation *in vivo* and *in vitro* as well as increasing the production of inflammatory cytokines and chemokines (*i.e.* IL-6, TNF-α, MIP-2, and MCP-1/5). More importantly, silencing the endogenous miR-873 or A20 gene with lentiviral vector of miR-873 sponge (LV-miR-873 sponge) or short hairpin RNA (shRNA) of A20 (LV-A20 shRNA) *in vivo* significantly lessened or aggravated inflammation and demyelination in the central nervous system (CNS) of EAE mice, respectively. Taken together, these findings indicate that miR-873 induced by IL-17 stimulation promotes the production of inflammatory cytokines and aggravates the pathological process of EAE mice through the A20/NF-κB pathway, which provides a new insight into the mechanism of inflammatory damage in MS.

Multiple sclerosis (MS),[2] a chronic autoimmune disease of the central nervous system (CNS) affecting young adults, is one of the foremost causes of non-traumatic neurological disability in young people. Reportedly, MS is driven by myelin-specific autoreactive T cells that infiltrate into the CNS and mediate an inflammatory response, resulting in demyelination and axon degradation (1, 2).

Strong evidence suggests that T helper 17 (Th17) cells are involved in various autoimmune and inflammatory diseases (3, 4). In MS, Th17 cells migrate across the blood-brain barrier into the CNS more efficiently than Th1 cells (5, 6). It has been revealed that IL-17, a signature cytokine produced by Th17, mediates the inflammatory response by recruiting immune cells and facilitating proinflammatory cytokine production (7), and IL-17 levels are notably elevated in MS, asthma, inflammatory bowel disease, psoriasis, and rheumatoid arthritis (4, 8). Moreover, the blockade of IL-17 signaling in mouse astrocytes attenuates the CNS injuries in experimental autoimmune encephalomyelitis (EAE; a widely used animal model of MS) (9).

Astrocytes, the major glial cell type within the CNS, regulate neuronal function and participate in the formation of the blood-brain barrier (10). Furthermore, astrocytes have the capacity to interact with the peripheral immune system by recruiting leukocytes into the CNS (11). In response to IL-6 and IL-17 treatment, astrocytes increase chemokine production to facilitate T cell recruitment to the CNS (12). However, the mechanisms by which astrocytes contribute to MS/EAE upon IL-17 stimulation remain unclear.

MicroRNAs (miRNAs), a class of non-coding RNA (~22 nucleotides in length), modulate gene expression by base pair-

* This work was supported by Jiangsu Province Key Laboratory of Neurodegeneration Grant SJ11KF07) and National Natural Science Foundation of China Grant 81072402 as well as the Priority Academic Program Development of Jiangsu Higher Education Institutions (PAPD).
[S] This article contains supplemental Figs. 1 and 2 and Tables 1–4.
[1] To whom correspondence should be addressed. Tel.: 86-25-86862769; Fax: 86-25-86508960; E-mail: wangyw1508@njmu.edu.cn.

[2] The abbreviations used are: MS, multiple sclerosis; miRNA, microRNA; EAE, experimental autoimmune encephalomyelitis; p-NF-κB, phospho-nuclear factor-κB; MOG, myelin oligodendrocyte glycoprotein; PDTC, pyrrolidine dithiocarbamate; ctrl shRNA, scrambled control shRNA; LFB, luxol fast blue; NC, negative control; LV, lentiviral; Th17, T helper 17.

ing with specific sequences in the 3′-UTR of target mRNAs, causing the degradation of mRNA or the inhibition of translation (13). Recently, the expression of several miRNAs has been identified and demonstrated to be up-regulated in mononuclear cells of peripheral blood or active lesions derived from patients with relapsing-remitting MS and EAE mice (13–16). However, the expression profiles and functions of miRNAs both in the brain tissue of EAE mice and in the astrocytes stimulated with IL-17 are still unknown.

The ubiquitin-editing enzyme A20 (TNFα-induced protein 3, TNFAIP3) is a widely inducible cytoplasmic protein that negatively regulates NF-κB-driven gene expression (17, 18). The NF-κB-driven astrocyte activation contributes to a more severe course of EAE (19). It is now recognized that A20, as a central regulator of inflammation, is associated with several autoimmune disorders, including MS (20).

In the present study, we found changes in the miRNA profiles both in the brain tissue of EAE mice (*in vivo*) and in the astrocytes exposed to IL-17 (*in vitro*). We selected miR-873, a co-up-regulated miRNA *in vivo* and *in vitro*, to further explore its function and mechanism in regulating the production of some cytokines (*i.e.* IL-6, TNF-α, MIP-2 (macrophage inflammatory protein-2), and MCP-1/5 (monocyte chemotactic protein-1/5)) and lesions of EAE mice. Our work revealed that miR-873 facilitated the production of inflammatory cytokines and chemokines in astrocytes stimulated with IL-17 by directly targeting and inhibiting A20 expression and indirectly promoting NF-κB activation. Silencing either miR-873 or A20 both *in vitro* and *in vivo* decreased or increased the production of these cytokines and ameliorated or aggravated the CNS damage of EAE mice, respectively. Our findings suggest that targeting certain miRNAs in astrocytes might be an important option to combat MS and EAE.

EXPERIMENTAL PROCEDURES

Animals—C57BL/6 mice were obtained from the Nanjing University Laboratory Animal Center. Protocols for animal experiments were approved by the Institutional Animal Use Committee of the Shanghai Institutes for Biological Sciences (Chinese Academy of Sciences). All mice were bred and housed under the care of the animal resources program.

Antibodies, Peptides, and Cells—Antibodies for mouse monoclonal anti-A20 (sc-166692), anti-β-actin (sc-47778), and rabbit polyclonal anti-RORγt (sc-28559) were from Santa Cruz Biotechnology, Inc.; rabbit polyclonal anti-p-NF-κB p65/Ser-536 was from Santa Cruz Biotechnology (sc-33020) or Cell Signaling Biotechnology (3033s); rabbit polyclonal anti-NF-κB (8242s) was obtained from Cell Signaling Biotechnology; and rabbit polyclonal anti-phospho-IKBα Ser-32/36 (BS4105) was provided by Bioworld Technology. The secondary antibodies were goat anti-mouse IgG and goat anti-rabbit IgG (Sigma). Myelin oligodendrocyte glycoprotein (MOG) amino acids 35–55 (MOG(35–55) peptide, MEVGWYRSPFSRVVHLYRNGK) were purchased from CL Bio-scientific Co. Ltd. (China).

Induction and Clinical Evaluation of EAE—EAE was induced in 6–8-week-old C57BL/6 female mice by subcutaneous immunization with 200 μg of MOG(35–55) emulsified in complete Freund's adjuvant (Sigma) containing 5 mg/ml heat-killed *Mycobacterium tuberculosis* (H37Ra strain, Difco). In addition, 200 ng of pertussis toxin (Invitrogen) in PBS was injected intraperitoneally on day 0 and day 2 after MOG(35–55) treatment. The immunization procedure of MOG(35–55) was repeated once on day 7 after the initial administration. Mice were monitored daily for clinical signs of EAE and graded on a scale of increasing severity from 0 to 5, according to a previously published grading scale (21): 0, no clinical signs; 1, limp tail; 2, paraparesis (weakness, incomplete paralysis of one or two hind limbs); 3, paraplegia (complete paralysis of two hind limbs); 4, paraplegia with fore limb weakness or paralysis; 5, moribund state or death. The same volume of PBS was injected into a parallel group of mice as into the negative control.

Primary Astrocyte Cultures—Primary astrocyte cultures from 0–1-day-old C57BL/6 mice were established as described previously with minor modifications (22). In brief, the cerebral cortices freed of meninges were dissected, minced, and digested. After being washed twice in Dulbecco's modified Eagle's medium/F-12 (DMEM/F-12) containing 10% fetal bovine serum (FBS) and antibiotics, the cells were filtrated through a 75-μm cell strainer and transferred to culture flasks precoated with 1 mg/ml poly-L-lysine (Sigma) and cultured at 37 °C with 5% CO_2. Complete confluence was reached in 7–9 days, and flasks were then shaken on an orbital shaker for 1 h (150 rpm at 37 °C). These cultures were continued for three or four passages and contained at least 95% positive cells of glial fibrillary acidic protein, as determined by immunofluorescent microscopy.

Real-time PCR—The total RNA from the brains of mice and cultured astrocytes was extracted with TRIzol reagent (Invitrogen). First-strand cDNAs were generated using the PrimeScript^{TM} RT reagent kit (TaKaRa, Otsu, Japan), and SYBR Premix Ex Taq^{TM}-based real-time PCR (TaKaRa) was used to analyze the relative expression levels of the following genes with different primer sets indicated: IL-17, 5′-CTC AGA CTA CCT CAA CCG TTC-3′ (forward) and 5′-TGA GCT TCC CAG ATC ACA GAG-3′ (reverse); IL-6, 5′-CCA CGG CCT TCC CTA C-3′ (forward) and 5′-AAG TGC ATC ATC GTT GT-3′ (reverse); TNF-α, 5′-CAT CTT CTC AAA ATT CGA GTG ACA A-3′ (forward) and 5′-TGG GAG TAG ACA AGG TAC AAC CC-3′ (reverse); MIP-2, 5′-GCC CCT CCC ACC TGC CGG CTG C-3′ (forward) and 5′-CTG AAC CAG GGG GGC TTC AGG G-3′ (reverse); MCP-1, 5′-AGA GAG CCA GAC GGA GGA AG-3′ (forward) and 5′-GTC ACA CTG GTC ACT CCT AC-3′ (reverse); MCP-5, 5′-GGA AGC TGA AGA GCT ACA GGA GAA-3′ (forward) and 5′-GAA GGT TCA AGG ATG AAG GTT TGA-3′ (reverse); GAPDH, 5′-CCT TCA TTG ACC TCA ACT AC-3′ (forward) and 5′-GGA AGG CCA TGC CAG TGA GC-3′ (reverse). The miRCURY LNA Universal RT microRNA PCR system (Exiqon) was used in conjunction with real-time PCR and SYBR Green Supermix (Roche Applied Science) for quantifying miRNA transcripts. U6 snRNA was used as an internal control with the following primers: 5′-CGC TTC GGC AGC ACA TAT AC-3′ (forward) and 5′-TTC ACG AAT TTG CGT GTC AT-3′ (reverse). The relative gene expression was calculated using the $2^{-\Delta\Delta CT}$ method.

ELISA—The levels of IL-17, IL-6, TNFα, MIP-2, and MCP-1/5 in the peripheral blood of mice or supernatants of cultured

astrocytes were detected using an IL-17 ELISA kit (BioLegend) or an IL-6, TNFα, MIP-2, and MCP-1/5 ELISA kit (eBioscience) according to the manufacturer's instructions.

Western Blot—As described previously (23), equal amounts of protein from the mouse brain tissue or the cultured astrocytes were separated on SDS-polyacrylamide gels, transferred to PVDF membrane, and probed with specific antibodies for RORγt, A20, p-NF-κB/p65, NF-κB, and phospho-IKBα. The expression of β-actin was used as a loading control.

miRNA Microarray Analysis and miRNA Target Prediction—The total RNA from the mouse brain tissue and astrocytes was extracted using TRIzol reagent and the RNeasy minikit (Qiagen) and was labeled with Hy3 fluorescent dyes. Labeled samples were hybridized to miRCURY LNA™ microRNA array slides with a coverage of 744 unique mouse microRNAs (Exiqon, 208301-A) using the miRCURY LNA™ Power labeling kit and the miRCURY LNA™ microRNA array kit (Exiqon). The median normalization method was used to obtain "normalized data," and normalized data = (foreground − background)/median. The full-length 3′-UTR of mouse A20 (BC060221.1) was obtained from the NCBI database, and miRNA sequences were obtained from miRBase. Four prediction programs (miRanda, TargetScan, PicTar, and RNAhybrid) were used to assess potential target sites for miRNA.

miRNA Mimics and miR-873 Inhibitor Synthesis—miRNA mimics and negative control of miRNA mimics (miR-NC) were synthesized by GenePharma with the following sequences: miR-323–5p mimics, 5′-AGG UGG UCC GUG GCG CGU UCG C-3′; miR-139–5p mimics, 5′-UCU ACA GUG CAC GUG UCU CCA G-3′; miR-763mimics, 5′-CCA GCU GGG AAG AAC CAG UGG C-3′; miR-873 mimics, 5′-GCA GGA ACU UGU GAG UCU CCU-3′; miR141 mimics, 5′-UAA CAC UGU CUG GUA AAG AUG G-3′; miR-NC mimics, 5′-UUG UAC UAC ACA AAA GUA CUG-3′. The miRCURYLNA™ inhibitor for miR-873 (LNA-anti-miR-873, 5′-AGG AGA CTC ACA AGT TCC T-3′) was obtained from Exiqon.

3′-UTR Plasmid Construction and Luciferase Reporter Assays—The full-length 3′-UTR of A20 was amplified and cloned into the pGL3-Promoter vector (Promega) at the XbaI restriction site. Mutations of A20 3′-UTR were introduced into the miRNA-binding sites by the QuikChange mutagenesis kit (TaKaRa). Using the Neon™ electrotransfection system, astrocytes or HEK293T cells were transfected with the pGL3-Promoter luciferase vector containing wild-type A20 3′-UTR (pGL3-Promoter/WT A20) or mutant A20 3′-UTR (pGL3-Promoter/Mut A20) accompanied by miR-323-5p, miR-139-5p, miR-763, miR-873, miR-141, and mutant miR-873, respectively. As previously described, luciferase activity was determined using the Dual-Luciferase assay system (Promega) at 48 h after transfection. Experiments were performed at least in triplicate, and the luciferase activity was normalized to *Renilla* luciferase activity (24).

Lentiviral miR-873 Construction—A genomic sequence spanning the mouse miR-873 coding region or miR-873-specific inhibitory oligonucleotide (miR-873 sponge) was cloned into the lentiviral vector pGLV-H1-GFP. A woodchuck hepatitis post-transcriptional regulatory element (WPRE) was also incorporated for optimal gene expression, and all constructs were verified by sequencing.

A20 shRNA Expression Plasmids and Lentiviral Vector Construction—To silence the mouse A20 gene, three different shRNA sequences against A20 mRNA were designed. The different plasmids of A20 shRNA were constructed using pGPU6/GFP, and the most effective shRNA expression plasmid was chosen for further experiments. Meanwhile, the scrambled control shRNA (ctrl shRNA) expression plasmid was used as a negative control. In addition, A20 shRNA or ctrl shRNA was cloned into the pGLV-H1-GFP lentiviral vector.

Histopathology—Mice were perfusion-fixed with 4% paraformaldehyde in 0.1 M sodium phosphate buffer (pH 7.4) under anesthesia. Brains and spinal cords were removed quickly and further fixed with the same fixation solution overnight at 4 °C. With light microscopy, the histological evaluation of brains and spinal cord tissues was performed on 4-μm paraffin-embedded sections stained with hematoxylin and eosin (H&E) or luxol fast blue (LFB) to assess inflammation and demyelination. For immunofluorescent staining, frozen sections (20 μm) from brain tissue were incubated with anti-A20 (Abcam) and anti-glial fibrillary acidic protein (Abcam). Immunohistochemistry for A20 and p-NF-κB on the mouse tissue sections was performed as described previously (23). For electron microscopy (EM), ultrathin sections of brains and spinal cord tissues were stained with uranyl acetate and lead citrate, and the ultrastructural changes were observed (24).

Statistical Analysis—Statistical analysis was performed with GraphPad Prism version 5.0 software using the two-tailed unpaired Student's *t* test or one-way multiple-range analysis of variance. A Mann-Whitney test was used for nonparametric data (EAE scoring). Values are expressed as the means ± S.E. A p value of <0.05 was considered significant.

RESULTS

Changes of IL-17, A20, and p-NF-κB Expression in the Brain Tissue of EAE Mice—Recent studies on MS patients and EAE mice have confirmed that Th17/IL-17 is involved in inflammatory injury (8, 25). To assess the role of Th17 cells and the levels of IL-17 and several inflammatory cytokines and chemokines in the EAE mice, we first induced EAE in mice and scored on a daily basis (Fig. 1*A*) and then detected the RORγt expression at different times in the brain tissue of EAE mice induced by MOG(35–55). Meanwhile, the production of IL-17, IL-6, TNF-α, MIP-2, and MCP-1/5 in the brain tissue and peripheral blood of EAE mice was detected by real-time PCR and ELISA, respectively. The results showed that the expression of RORγt was significantly increased on day 14 after MOG(35–55) immunization and then gradually elevated until day 20 compared with negative control (NC) groups (Fig. 1*B*). The expression of IL-17 mRNA and protein began to increase on day 7 after administration of MOG(35–55). On day 20, the level of IL-17 was significantly enhanced (Fig. 1, *C* and *D*). Meanwhile, EAE scoring reached an average of 4.0. Similarly, the production of IL-6, TNF-α, MIP-2, and MCP-1/5 in EAE mice was also up-regulated following the development of EAE (supplemental Fig. 1, *A* and *B*). Subsequently, we examined the levels of A20 expression and NF-κB activation in EAE mice. Western blot analysis indicated that the level of A20 protein was decreased in the brain tissue of EAE mice on day 14 and was even lower on

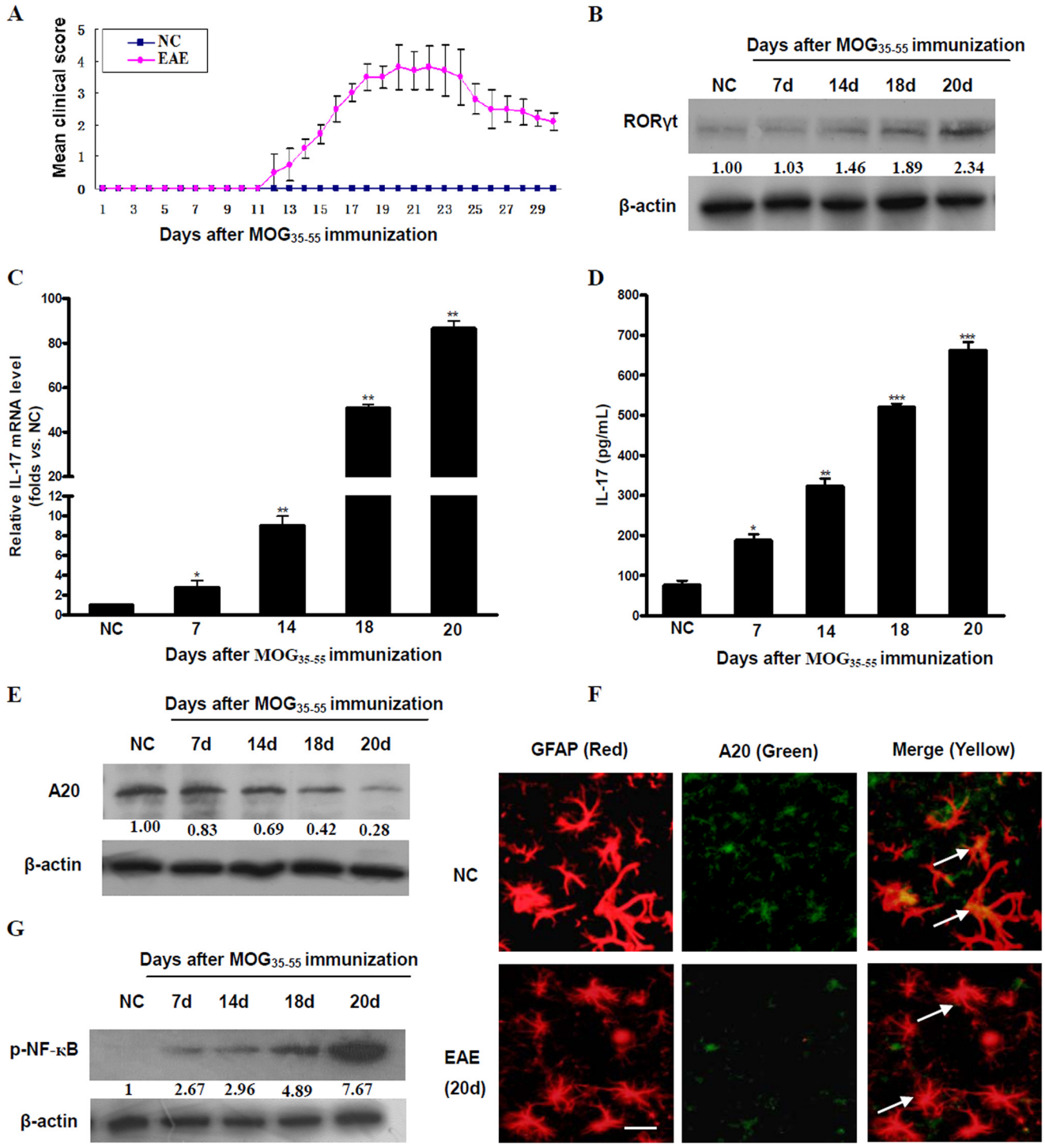

FIGURE 1. **Kinetic changes of IL-17, A20, and p-NF-κB/p65 expression during EAE induction.** The EAE model of C57BL/6 female mice was established by MOG(35–55) immunization. *A*, the clinical grades were evaluated for 30 days in mice immunized by MOG(35–55) ($n = 10$ mice/group). *B*, expression of RORγt in the brain tissue was analyzed by a Western blot assay. *β*-Actin was used as an internal control for the protein level. *C* and *D*, the level of IL-17 in the brain tissue and peripheral blood of EAE mice was measured using real-time PCR and ELISA, respectively. GAPDH was used as an internal control. *E*, Western blot analysis showed that A20 protein expression in the mouse was reduced on day 14 after MOG(35–55) immunization and was significantly lower on day 20 compared with NC groups. *F*, immunofluorescent (*IF*) staining of A20 and glial fibrillary acidic protein (*GFAP*) in the brain tissue of NC mice and EAE mice immunized by MOG(35–55) for 20 days. *Scale bars*, 50 μm. *G*, the phosphorylation of NF-κB (p-NF-κB/p65) was increased on day 7 after MOG(35–55) treatment and was higher than that of NC groups. *, $p < 0.05$; **, $p < 0.01$; ***, $p < 0.001$ *versus* NC groups ($n = 4$ mice/group). *Error bars*, S.E.

day 20 after MOG(35–55) immunization (Fig. 1*E*). Moreover, immunofluorescent staining showed that A20 protein was expressed in the brain astrocytes, and its level was reduced 20 days after MOG(35–55) immunization (Fig. 1*F*). In contrast, the phosphorylation of NF-κB (p-NF-κB/p65 expression) showed a time-dependent increase and reached a higher level in the brain tissue of mice on day 20 after MOG(35–55) immunization (Fig. 1*G*).

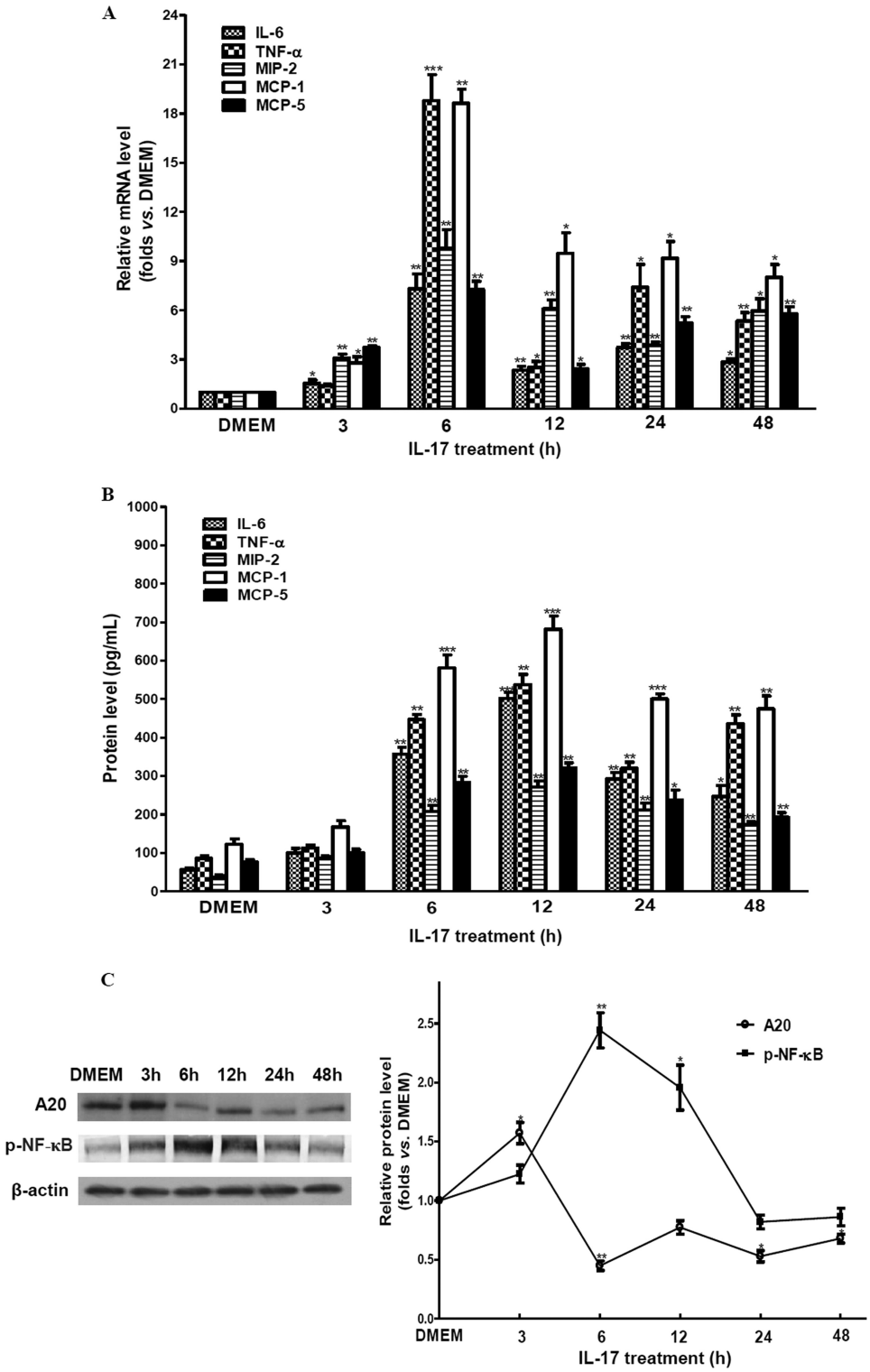

FIGURE 2. **The production of IL-6, TNF-α, MIP-2, and MCP-1/5 and the expression of A20 and p-NF-κB in astrocytes with IL-17 treatment.** Mouse brain primary astrocytes were cultured in a serum-free DMEM/F-12 medium overnight followed by stimulation with IL-17 for various time periods, and then the mRNA and protein levels of cytokines in astrocytes and culture supernatants were detected using real-time PCR and ELISA, respectively. *A* and *B*, time courses of IL-6, TNF-α, MIP-2, and MCP-1/5 mRNA and protein levels in astrocytes stimulated by IL-17 at different time points. *C*, the expression of A20 protein and the level of p-NF-κB in the astrocytes stimulated with IL-17 were examined using a Western blot assay. *, $p < 0.05$; **, $p < 0.01$; ***, $p < 0.001$ *versus* DMEM groups. Data are from three independent experiments. *Error bars*, S.E.

Production of IL-6, TNF-α, MIP-2, and MCP-1/5 and the Expression of A20 and p-NF-κB in the Astrocytes in Response to IL-17 Stimulation—The primary astrocytes of C57BL/6 mice were stimulated with recombinant mouse IL-17 (50 ng/ml; R&D Systems; dose dependent on IL-17 stimulation (see supplemental Fig. 2)) in serum-free media for different times. The time course data showed that the mRNA levels of IL-6, TNF-α, MIP-2, and MCP-1/5 were significantly increased and reached

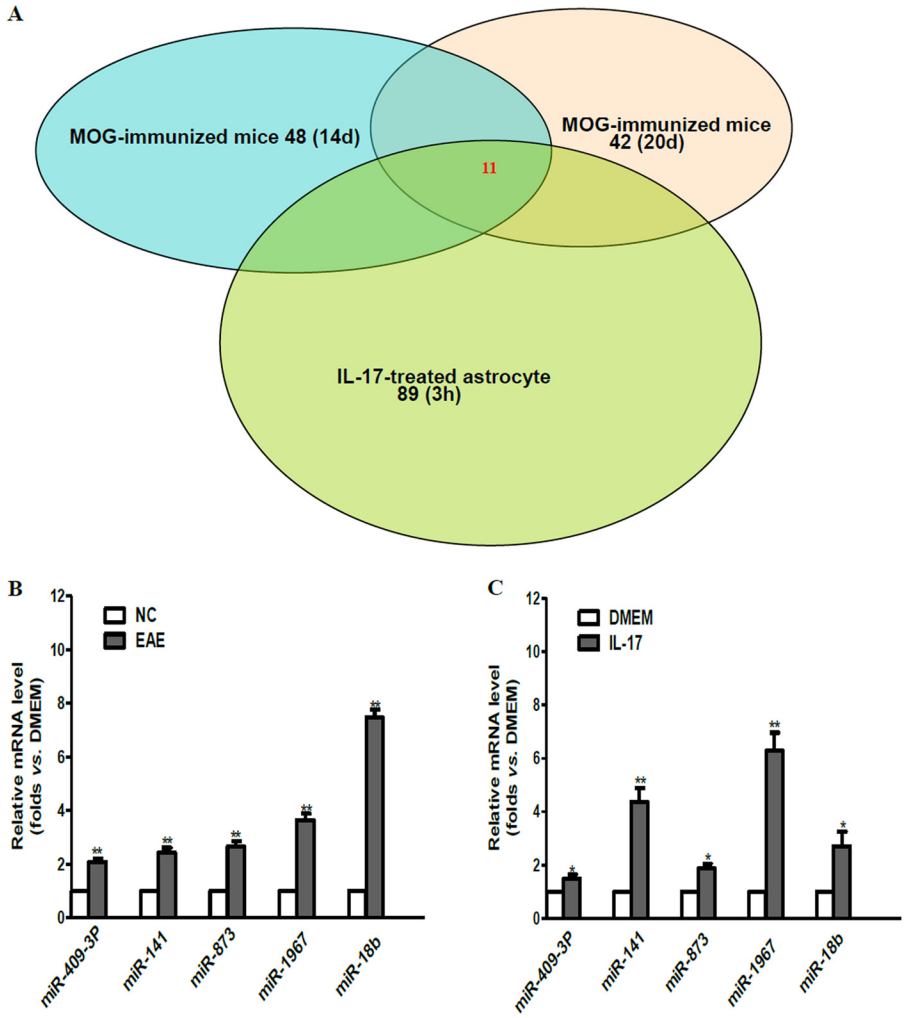

FIGURE 3. **Analysis of up-regulated miRNA profiles in the brain tissue of EAE mice and in the astrocytes upon IL-17 stimulation.** *A*, comparative microarray analysis indicated that 48 miRNAs on day 14 and 42 miRNAs on day 20 were up-regulated (1.5-fold higher than NC group) in the brain tissue of mice after MOG(35–55) immunization, and 89 miRNAs were up-regulated at 3 h in the primary astrocytes with IL-17 treatment. Specifically, 11 miRNAs were differentially co-up-regulated in the above three groups. *B* and *C*, real-time PCR analysis for five miRNAs among the 11 miRNAs showed that these miRNAs occurred in higher levels both *in vivo* and *in vitro* compared with NC or DMEM controls. *, $p < 0.05$; **, $p < 0.01$ *versus* NC or DMEM groups ($n = 3$ mice/group). U6 snRNA was a loading control. *Error bars*, S.E.

TABLE 1

Identification of 11 miRNAs that are differentially up-regulated both in the brain tissue of EAE mice and in the astrocytes stimulated with IL-17 for 3 h

miRNA name	MOG(35–55) immunized for 14 days	MOG(35–55) immunized for 20 days	IL-17 stimulation for 3 h
	-fold up-regulated	*-fold up-regulated*	*-fold up-regulated*
mmu-miR-31	1.81381	2.16235	1.76824
mmu-miR-18b	3.02376	5.28367	2.90983
mmu-miR-141	4.85634	2.11347	5.59348
mmu-miR-666–3p	1.84785	3.69857	5.54253
mmu-miR-449b	6.04751	2.11347	4.67651
mmu-miR-449c	1.51188	5.28367	2.77127
mmu-miR-1967	2.68778	2.46571	7.49727
mmu-miR-873	1.51940	1.67472	1.73204
mmu-miR-145	1.56833	1.59950	1.67456
mmu-miR-409-5p	2.34623	2.16116	1.67632
mmu-miR-409-3p	1.61827	1.64381	2.20608

their peak at 6 h after IL-17 stimulation in astrocytes (Fig. 2*A*). Meanwhile, the secretion of inflammatory cytokines and chemokines in the culture supernatants also increased at 6 h after IL-17 treatment and peaked at 12 h (Fig. 2*B*). Furthermore, the expression of A20 protein at 6 h in the astrocytes in response to IL-17 stimulation showed a significant decrease, whereas the phosphorylation level of NF-κB (p-NF-κB/p65) displayed a significant increase (Fig. 2*C*). Taken together, the results *in vitro* indicated that the mouse astrocytes exposed to IL-17 increased the production of IL-6, TNF-α, MIP-2, MCP-1/5, and p-NF-κB/p65 and decreased the expression of A20 protein.

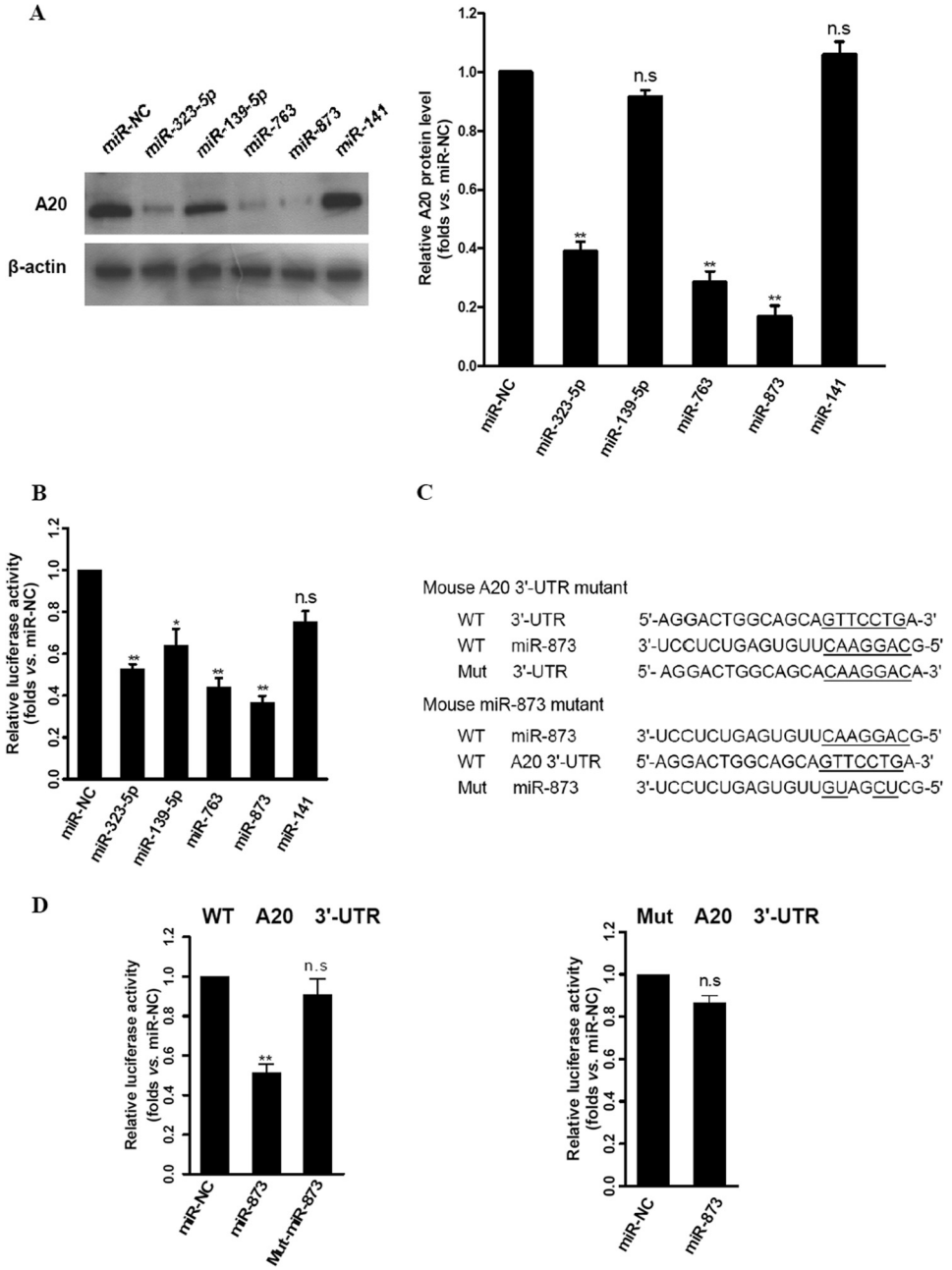

FIGURE 4. **Screening and identification of miRNAs targeted A20 gene.** *A*, mouse primary astrocytes were transfected with predicted miRNAs (miR-323-5p, miR-139-5p, miR-763, miR-873, and miR-141) complementary to A20 3′-UTR using the Neon^{TM} electron transfection system for 48 h, and the expression of A20 in astrocytes was detected by a Western blot assay. Results showed that the protein level of A20 was significantly reduced (**, $p < 0.01$) in astrocytes transfected with miRNA mimics (miR-323–5p, miR-763, and miR-873) compared with the control miRNA mimics (miR-NC), especially miR-873. *B*, the astrocytes were transfected with the luciferase reporter containing WT A20 3′-UTR (pGL3-Promoter/WT A20) accompanied by the transfection of the above miRNAs for 48 h. The luciferase activity of pGL3-Promoter/WT A20 was significantly suppressed in miR-323–5p, miR-763, and miR-873 groups compared with miR-NC groups (*, $p < 0.05$; **, $p < 0.01$). *C*, sequences of mutations in A20 3′-UTR (Mut A20 3′-UTR) or in miR-873 seed sequences binding to A20 (Mut miR-873). *D*, the astrocytes were co-transfected with WT miR-873 or Mut miR-873 accompanied by the pGL3-Promoter/WT A20 vector as well as with WT miR-873 with the pGL3-Promoter/Mut A20 vector. The luciferase activity of the respective corresponding vector was analyzed. **, $p < 0.01$ *versus* miR-NC groups. Data are from three independent experiments. *Error bars*, S.E.

Analysis of miRNA Expression Profiles in the Brain Tissue of EAE Mice and in the Astrocytes Stimulated with IL-17—Recent studies have revealed that miRNAs can regulate the production of cytokines both in MS patients and EAE mice (15, 16, 26, 27). However, the changes of miRNA expression profiles both in the brain tissue of EAE mice (*in vivo*) and in the astrocytes upon IL-17 stimulation (*in vitro*) remain unclear. We used an miRNA microarray to identify the miRNA expression profiles in the brains of the EAE mice after MOG(35–55) immunization on day 14 and day 20 and in the cultured primary astrocytes stimulated with IL-17 at 3 and 6 h. The data showed that 90 miRNAs were up-regulated (at least 1.5-fold higher than NC mice), and 42 miRNAs were down-regulated (at least 0.5-fold lower than NC mice) in the brain tissue of EAE mice. Meanwhile, 98 miRNAs (89 miRNAs at 3 h and 9 miRNAs at 6 h) were up-regulated (at least 1.5-fold higher than DMEM control groups), and 62

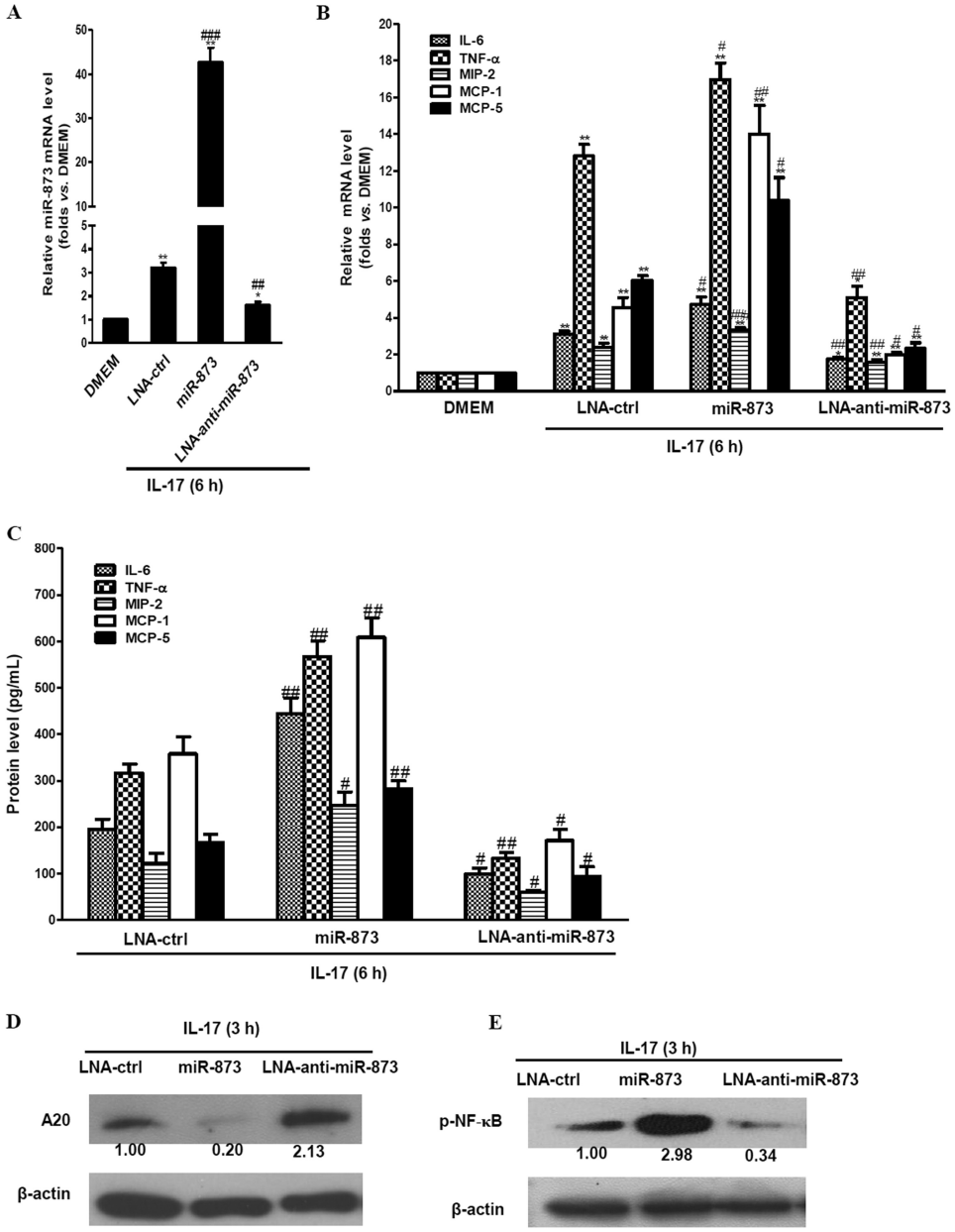

FIGURE 5. **The role of miR-873 in the production of IL-6, TNF-α, MIP-2, and MCP-1/5; the expression of A20 protein; and the level of p-NF-κB in astrocytes with IL-17 treatment.** Primary astrocytes were transfected with LNA-ctrl, miR-873 mimics, or LNA-anti-miR-873 (miR-873 inhibitor) for 48 h. Thereafter, the cells were subjected to IL-17 stimulation for 6 h. *A*, the astrocytes transfected with miR-873 mimics or LNA-anti-miR-873 showed greater or lower mRNA expression of miR-873 compared with LNA-ctrl groups, respectively. Measured transcript levels were normalized to U6 snRNA expression. *B* and *C*, the mRNA and protein levels of IL-6, TNF-α, MIP-2, MCP-1, and MCP-5 in the astrocytes transfected with LNA-ctrl, miR-873 mimics, or LNA-anti-miR-873 were analyzed using real-time PCR and ELISA, respectively. *D*, the astrocytes were transfected with LNA-ctrl, miR-873 mimics, or LNA-anti-miR-873 for 48 h, separately, and then stimulated with IL-17 for 3 h. The protein level of A20 in the astrocytes transfected with miR-873 mimics was significantly decreased compared with LNA-ctrl groups by Western blot analysis. *E*, a remarkable elevation of the phosphorylation of NF-κB (p-NF-κB/p65) was identified in the astrocytes transfected with miR-873 mimics. *, $p < 0.05$; **, $p < 0.01$ *versus* DMEM groups; #, $p < 0.05$; ##, $p < 0.01$; ###, $p < 0.001$ *versus* LNA-ctrl groups. Results are represented as mean ± S.E. (*error bars*).

miRNAs were down-regulated (at least 0.5-fold lower than DMEM control groups) in the astrocytes after IL-17 stimulation (examples of up-regulated or down-regulated miRNAs *in vivo* and *in vitro* are shown in supplemental Tables 1–4). Notably, there were 11 miRNAs that differentially co-up-regulated both in the brain tissue of EAE mice and in the astrocytes stimulated with IL-17 for 3 h (Fig. 3*A* and Table 1). Of these co-up-regulated miRNAs, several miRNAs, such as miR-409-3p, miR-141, miR-873, miR-1967, and miR-18b, were also validated by real-time PCR (Fig. 3, *B* and *C*).

Screening and Identification of the miRNAs Complementary to A20 3′-UTR—The potential targets of miRNAs were predicted from several widely used prediction algorithms, including TargetScan, PicTar, miRanda, and RNAhybrid. Computational prediction indicated that the miRNAs (miR-323–5p, miR-139–5p, miR-763, miR-873, and miR-141) could bind to A20 3′-UTR. To investigate the role of these miRNAs in regulating A20, we transfected them using the Neon^{TM} transfection system (MPK5000) into mouse primary astrocytes. Western blot results showed that miR-323–5p, miR-763, and miR-873

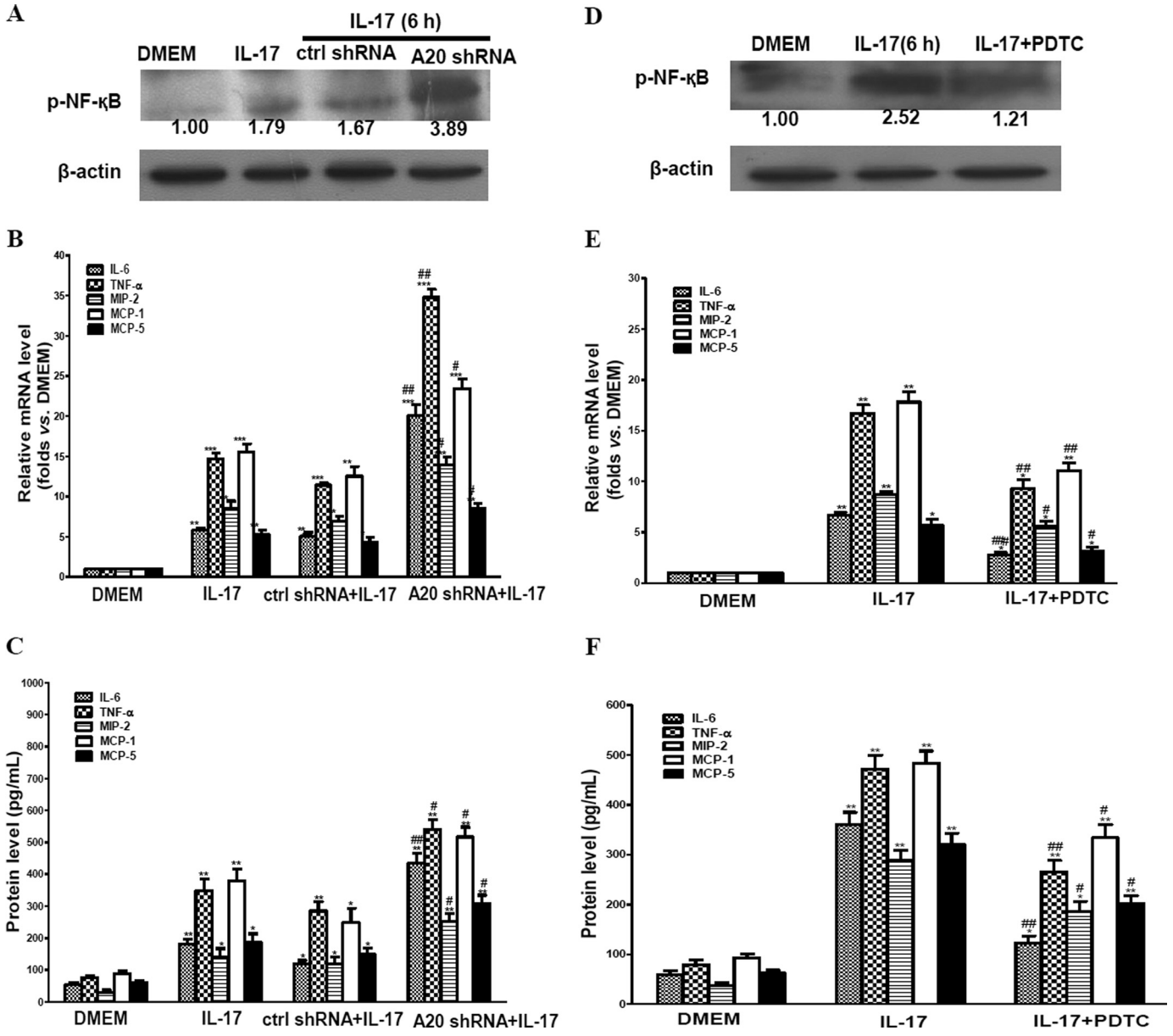

FIGURE 6. **The effects of A20 gene silencing and NF-κB activation suppression on the NF-κB activation and inflammatory cytokine production in astrocytes with IL-17 treatment.** *A–C*, mouse primary astrocytes were transfected with A20 shRNA and ctrl shRNA plasmid for 72 h, respectively. Then the astrocytes were stimulated with IL-17 for 6 h. The phosphorylation of NF-κB (p-NF-κB/p65) in A20 shRNA-transfected astrocytes was significantly stronger than that in IL-17 treatment alone using Western blot analysis (##, $p < 0.01$). Also, the levels of inflammatory cytokine expression and secretion in astrocytes were measured using real-time PCR and ELISA, respectively. *D–F*, the astrocytes were treated by PDTC (inhibitor of NF-κB activation; 25 μM) for 2 h and then stimulated with IL-17 for 6 h. The increased phosphorylation of NF-κB (p65) in the astrocytes stimulated by IL-17 was markedly diminished with Western blot analysis. Similar changes in the production of IL-6, TNF-α, MIP-2, and MCP-1/5 from the astrocytes were identified using real-time PCR and ELISA. *, $p < 0.05$; **, $p < 0.01$; ***, $p < 0.001$ *versus* DMEM groups. #, $p < 0.05$; ##, $p < 0.01$ *versus* IL-17 treatment alone groups. Results are represented as mean ± S.E. (*error bars*) ($n = 3$ mice/group).

reduced A20 protein expression compared with the miRNA control mimics (negative control), especially miR-873 (Fig. 4*A*). At the same time, we cloned 3′-UTR of the mouse wild-type (WT) A20 gene into the luciferase reporter vector (pGL3-Promoter/WT A20). The co-transfection of these miRNAs with pGL3-Promoter/WT A20 to astrocytes resulted in a significant suppression of luciferase activity of pGL3-Promoter/WT A20 reporter by miR-323–5p, miR-763, and miR-873, whereas the co-transfection of the negative control miRNA did not show any effects on luciferase activity (Fig. 4*B*). Considering that the down-regulation of A20 expression in astrocytes by miR-873 was much stronger than that of other miRNAs, we selected miR-873 for further study. Additionally, to verify the specificity of miR-873-mediated A20 repression, the putative binding sites of the A20 3′-UTR and miR-873 seed region were mutated. The 3′-UTR of mouse A20 gene contains a 7-mer (GTTCCTG), which is perfectly complementary to the seed region of miR-873 (Fig. 4*C*). In mouse primary astrocytes, the co-transfection of miR-873 with pGL3-Promoter/WT A20 or pGL3-Promoter/Mut A20 reporter (a mutated A20 3′-UTR vector) showed that miR-873 significantly inhibited the luciferase activity of the pGL3-Promoter/WT A20 but not that of the pGL3-Promoter/

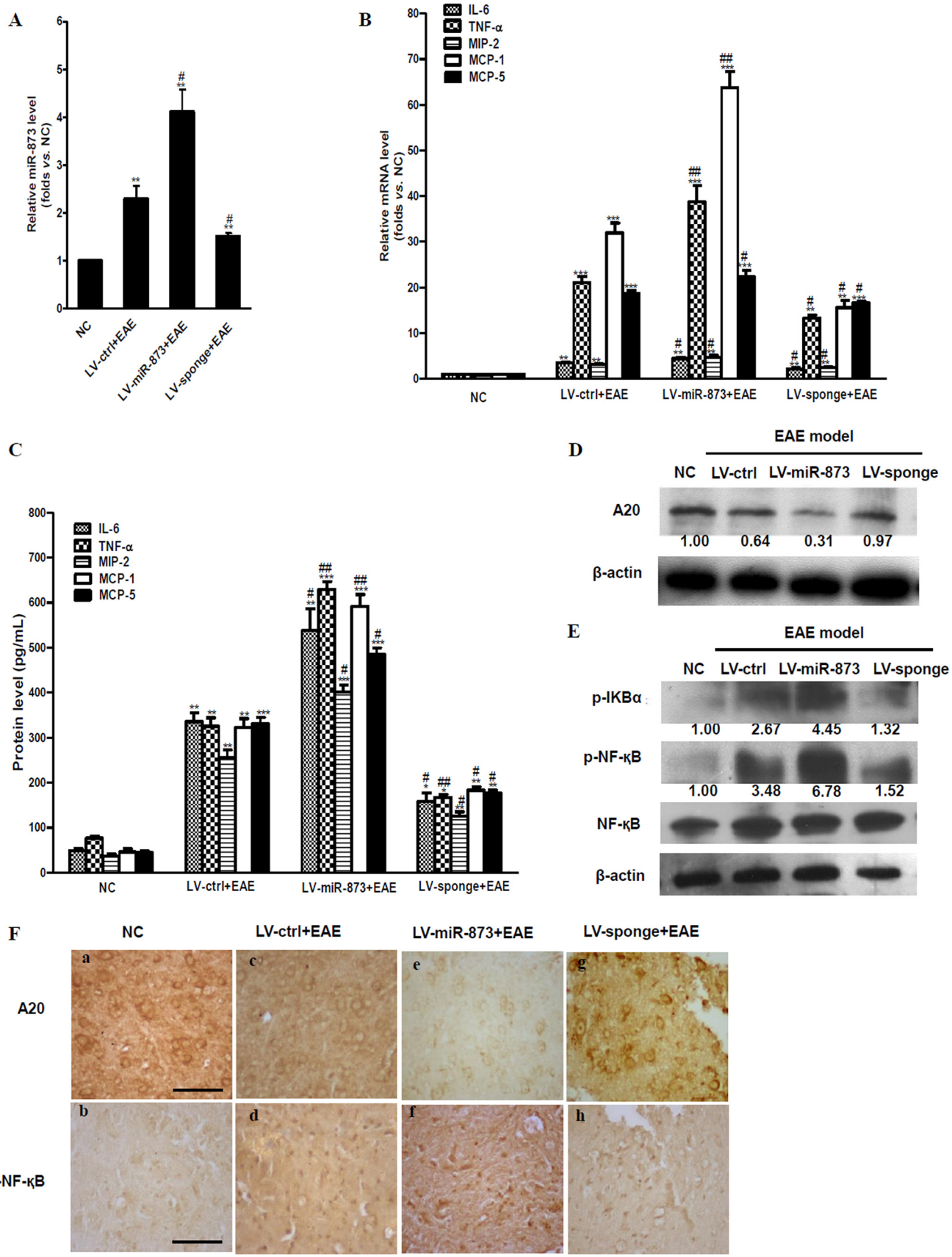
A
Relative miR-873 level (folds vs. NC)
NC
LV-ctrl+EAE
LV-miR-873+EAE
LV-sponge+EAE
B
IL-6
TNF-α
MIP-2
MCP-1
MCP-5
Relative mRNA level (folds vs. NC)
NC
LV-ctrl+EAE
LV-miR-873+EAE
LV-sponge+EAE
C
IL-6
TNF-α
MIP-2
MCP-1
MCP-5
Protein level (pg/mL)
NC
LV-ctrl+EAE
LV-miR-873+EAE
LV-sponge+EAE
D
EAE model
NC
LV-ctrl
LV-miR-873
LV-sponge
A20
1.00
0.64
0.31
0.97
β-actin
E
EAE model
NC
LV-ctrl
LV-miR-873
LV-sponge
p-IKBα
1.00
2.67
4.45
1.32
p-NF-κB
1.00
3.48
6.78
1.52
NF-κB
β-actin
F
NC
LV-ctrl+EAE
LV-miR-873+EAE
LV-sponge+EAE
A20
p-NF-κB
a
b
c
d
e
f
g
h

Mut A20 (Fig. 4*D*). Likewise, the astrocytes co-transfected with the mutated miR-873 either did not show decreased luciferase activity of the pGL3-Promoter/WT A20 reporter (Fig. 4*D*). Taken together, these data suggest that A20 is a functional target of miR-873.

The Effects of miR-873 on the Production of IL-6, TNF-α, MIP-2, and MCP-1/5 as Well as A20 and p-NF-κB in Astrocytes Stimulated with IL-17—In order to confirm that miR-873 up-regulated both *in vivo* and *in vitro* promotes the production of inflammatory cytokines in astrocytes after IL-17 stimulation, the mouse primary astrocytes were transfected with LNA-ctrl, miR-873 mimics, and LNA-anti-miR-873 (miR-873 inhibitor, locked nucleic acid anti-miR-873, Exiqon) for 48 h, respectively, and then stimulated with IL-17 for 6 h. The results showed that the astrocytes transfected with miR-873 had a 10-fold greater expression of mature miR-873, and those transfected with LNA-anti-miR-873 showed a 2-fold lower expression compared with the LNA-ctrl groups (Fig. 5*A*). Next, we examined the mRNA and protein levels of IL-6, TNF-α, MIP-2, and MCP-1/5 using real-time PCR and ELISA, respectively. As expected, the astrocytes transfected with miR-873 mimics or LNA-anti-miR-873 significantly increased or decreased the levels of IL-6, TNF-α, MIP-2, and MCP-1/5 production, respectively (Fig. 5, *B* and *C*). Moreover, the astrocytes transfected with miR-873 mimics and then stimulated with IL-17 for 3 h remarkably reduced the A20 expression while enhancing the p-NF-κB/p65 level, and LNA-anti-miR-873 reversed the changes of A20 and p-NF-κB/p65 expression by miR-873 mimics (Fig. 5, *D* and *E*). These data reveal that miR-873 plays a role in regulating the production of inflammatory cytokines and inflammation-related proteins in the astrocytes treated by IL-17.

The Effects of A20 on the Activation of NF-κB and the Production of IL-6, TNF-α, MIP-2, and MCP-1/5 in the Astrocytes Stimulated with IL-17—To prove that A20 can negatively modulate the NF-κB signaling pathways in astrocytes, we generated A20 shRNA plasmids using the pGPU6/GFP vector, and the most effective plasmid that could silence the A20 gene was chosen for further experiments. Thereafter, the mouse primary astrocytes were transfected with either A20 shRNA or the ctrl shRNA plasmids for 72 h, followed by IL-17 treatment for 6 h. After this treatment, the activation of NF-κB in astrocytes was investigated by Western blot. As shown (Fig. 6*A*), silencing A20 prior to IL-17 treatment in astrocytes remarkably enhanced the phosphorylation of NF-κB (p-NF-κB/p65) compared with IL-17 treatment alone. In addition, silencing A20 in astrocytes strongly increased IL-6, TNF-α, MIP-2, and MCP-1/5 production (Fig. 6, *B* and *C*). These findings suggest that A20 mediates NF-κB activation and the production of inflammatory cytokines in astrocytes. To further explore the potential signaling pathway of the inflammatory cytokine production in the astrocytes in response to IL-17, the effects of p-NF-κB on the synthesis of these cytokines in the astrocytes upon IL-17 were detected. The results showed that the astrocytes administrated with ammonium pyrrolidine dithiocarbamate (PDTC; inhibitor of NF-κB activation) at 2 h prior to the IL-17 stimulation markedly diminished the expression of p-NF-κB/p65 (Fig. 6*D*), including five cytokines described previously at 6 h after IL-17 treatment (Fig. 6, *E* and *F*). Together, these data imply that the production of inflammatory cytokines in the astrocytes stimulated by IL-17 is mediated by the miR-873/A20/NF-κB pathway.

The Roles of miR-873 in the Production of IL-6, TNF-α, MIP-2, MCP-1/5, A20, and p-NF-κB in EAE Mice—To further demonstrate the effects of miR-873 on the production of pro-inflammatory cytokines, A20, and p-NF-κB/p65 in EAE mice, the lentiviral (LV) expression vectors with green fluorescent protein (GFP) of LV-ctrl (a mutant miR-873 control), LV-miR-873 (encoding pre-miR-873), and LV-miR-873 sponge (antagonizing the endogenous miR-873 activity) were constructed and then injected into C57BL/6 mice through the tail vein. Briefly, the mice were injected with 5×10^7 transforming units/mouse of recombinant lentivirus. On day 7 after the recombinant lentivirus injection, the EAE model was induced by immunizing MOG(35–55) for 18 days. Then the efficacy of miR-873 expression in the brain tissue of miR-873-infected mice and LV-sponge-infected mice was separately assessed using real-time PCR. The results from frozen sections showed that the recombinant lentivirus could reach the CNS on day 7 after the recombinant lentivirus injection (data not shown). The mice infected with LV-miR-873 mimics or LV-sponge had a higher or lower expression of miR-873, respectively, in the brain compared with LV-ctrl groups (Fig. 7*A*). In addition, the overexpression of miR-873 in the brains of EAE mice treated with LV-miR-873 showed significantly increased levels of IL-6, TNF-α, MIP-2, and MCP-1/5. Conversely, the repression of the endogenous miR-873 in EAE mice infected with LV-sponge diminished the production of these inflammatory cytokines (Fig. 7, *B* and *C*). Similar changes were identified in the spinal cords of EAE mice treated with different lentivirus vectors (data not shown). Notably, the EAE mice injected with LV-miR-873 showed a markedly down-regulated A20 expression, but the mice with LV-sponge treatment reversed the decreased A20 level (Fig. 7*D*). In addition, the EAE mice administered with the LV-sponge substantially suppressed the phosphorylation of IKBα and NF-κB compared with the LV-ctrl groups, and there was no effect on NF-κB expression in the mice treated with LV-miR-873 or LV-sponge (Fig. 7*E*). To further investigate the roles of miR-873 in A20 and p-NF-κB/p65 production, the

FIGURE 7. **The effects of miR-873 on the production of inflammatory cytokines, the expression of A20 protein, and the level of p-NF-κB/p65 in EAE mice.** Mice were injected with various recombinant lentivirus (LV-control, LV-miR-873, or LV-sponge) for 7 days and then immunized with MOG(35–55) for 18 days ($n = 10$ mice/group). *A*, the EAE mice infected with LV-miR-873 or LV-sponge showed higher or lower miR-873 mRNA levels in the brain tissue compared with the LV-ctrl group. *B*, the EAE mice treated with LV-miR-873 or LV-sponge showed higher or lower mRNA levels of IL-6, TNF-α, MIP-2, and MCP-1/5 in the cells. *C*, the changes of these cytokines in the peripheral blood of the EAE mice in LV-control, LV-miR-873, and LV-sponge treatment groups by ELISA were similar to the changes of the corresponding mRNA in the brain tissue of the EAE mice. *D*, A20 expression in the mouse brain tissue was detected using a Western blot assay. The EAE mice administered with LV-miR-873 or LV-sponge had remarkably down-regulated or up-regulated A20 expression, respectively. *E*, the EAE mice infected with LV-miR-873 or LV-sponge notably increased or decreased the protein levels of both phospho-IKBα and p-NF-κB/p65 in the brain tissue, respectively. *F*, the immunohistochemical staining of A20 and p-NF-κB/p65 in the spinal cord of different groups, and examples showed that the mice treated with LV-sponge had significantly up-regulated A20 expression in cytoplasm, whereas p-NF-κB/p65 expression in the nucleus was down-regulated. *Scale bars*, 50 μm. *, $p < 0.05$; **, $p < 0.01$; ***, $p < 0.001$ *versus* NC groups. #, $p < 0.05$; ##, $p < 0.01$ *versus* LV-ctrl + EAE groups. *Error bars*, S.E.

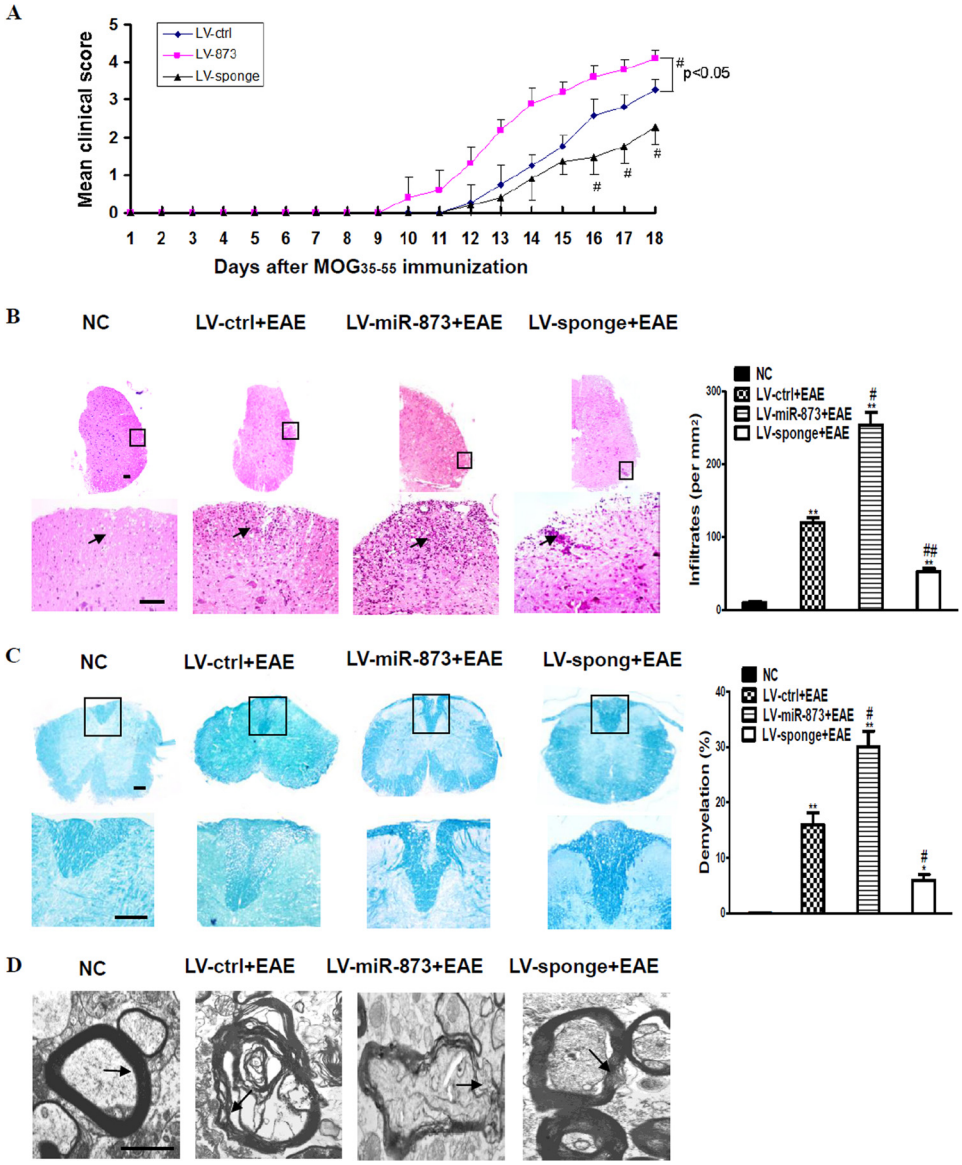

FIGURE 8. **The role of miR-873 in behavior and pathology of EAE mice.** On day 7 after the corresponding lentivirus administration (LV-ctrl, LV-miR-873, or LV-sponge), the mice were immunized with MOG(35–55) for 18 days. *A*, the clinical scores for EAE mice infected with different recombinant lentivirus ($n = 10$ mice/group). *B*, hematoxylin and eosin (H&E) staining of spinal cords isolated from mice. *Boxed areas* in the *top rows* are presented *enlarged below* (*scale bars*, 50 μm). *C*, severe damage of the medullary sheath in LV-miR-873-infected mice was observed by luxol fast blue (*LFB*) staining (*scale bars*, 50 μm). In LV-sponge-infected mice, demyelination was reduced compared with the LV-control group (quantification presents the demyelination area relative to total analyzed area). *D*, the spinal cords in LV-miR-873-infected mice or LV-sponge-infected mice under EM exhibited severe disruption or mild loosening of the medullary sheath compared with the LV-ctrl-infected mice, respectively ($n = 4$ mice/group). *Scale bars*, 1 μm. *, $p < 0.05$; **, $p < 0.01$ *versus* NC groups. #, $p < 0.05$; ##, $p < 0.01$ *versus* LV-ctrl + EAE groups. *Error bars*, S.E.

immunohistochemistry of A20 and p-NF-κB/p65 was performed in the spinal cords of EAE mice. As shown, strong A20 immunoreactivity in cytoplasms and weak p-NF-κB/p65 immunoreactivity in nuclei were found in NC mice (Fig. 7*F*, *a* and *b*). In EAE mice treated with LV-ctrl, A20 immunoreactivity was decreased, and p-NF-κB/p65 immunoreactivity was significantly increased (Fig. 7*F*, *c* and *d*). Moreover, the A20 immunoreactivity was lower and p-NF-κB/p65 immunoreactivity was higher in EAE mice treated with LV-miR-873, compared with EAE mice injected with LV-ctrl (Fig. 7*F*, *e* and *f*). However, in EAE mice treated with LV-sponge, the A20 immunoreactivity was reversed and significantly enhanced, whereas the p-NF-κB/p65 immunoreactivity was markedly inhibited (Fig. 7*F*, *g* and *h*). Collectively, these data imply that the production of inflammatory cytokines and chemokines in EAE mice is indeed regulated by the miR-873/A20/NF-κB pathway.

The Effects of miR-873 on Behavior and Pathology of EAE Mice—In a recent study, miR-326 expression was demonstrated to correlate with disease severity in MS patients and EAE mice (28). Mice with miR-155 deletions ($Mir155^{-/-}$) are highly resistant to EAE (27, 29). To further verify whether miR-873 contributes to the development and pathogenesis of EAE, we assessed the efficacy of miR-873 through the systemic administration of various lentivirus vectors *in vivo*. The results showed that the EAE mice infected with LV-miR-873 developed more severe EAE, whereas the EAE mice treated with LV-sponge had a delayed onset of EAE and had milder clinical behavior of EAE (Fig. 8*A*). In addition, spinal cord sections

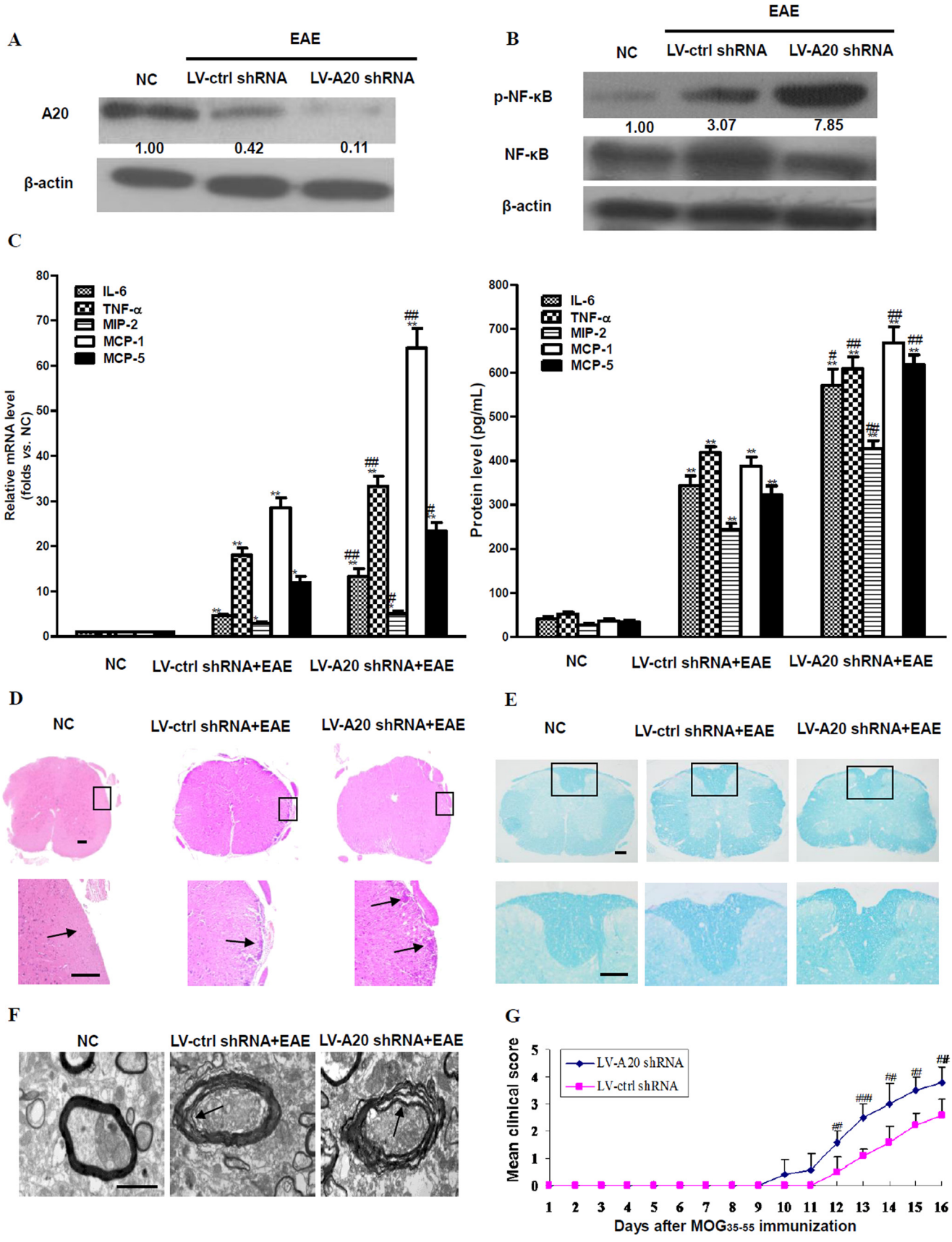
A
EAE
NC
LV-ctrl shRNA
LV-A20 shRNA
A20
1.00
0.42
0.11
β-actin
B
EAE
NC
LV-ctrl shRNA
LV-A20 shRNA
p-NF-κB
1.00
3.07
7.85
NF-κB
β-actin
C
IL-6
TNF-α
MIP-2
MCP-1
MCP-5
Relative mRNA level (folds vs. NC)
Protein level (pg/mL)
NC
LV-ctrl shRNA+EAE
LV-A20 shRNA+EAE
D
NC
LV-ctrl shRNA+EAE
LV-A20 shRNA+EAE
E
NC
LV-ctrl shRNA+EAE
LV-A20 shRNA+EAE
F
NC
LV-ctrl shRNA+EAE
LV-A20 shRNA+EAE
G
LV-A20 shRNA
LV-ctrl shRNA
Mean clinical score
Days after MOG35-55 immunization

showed that the EAE mice infected with LV-miR-873 developed prominent inflammatory cell infiltration, whereas the mice infected with LV-sponge had minor inflammation on day 18 after MOG(35–55) immunization (Fig. 8*B*). Similarly, LFB staining manifested that the mice treated with LV-miR-873 appeared to have severe demyelination, whereas the mice infected with LV-sponge had markedly lessened demyelination (Fig. 8*C*). Specifically, the myelin sheath of the EAE mice injected with LV-miR-873 was ruptured and disintegrated under EM, whereas only a mild loosening of the medullary sheath was seen in the EAE mice injected with LV-sponge (Fig. 8*D*). These findings indicate that the knockdown of miR-873 *in vivo* can ameliorate the pathological changes in EAE mice.

The Roles of A20 in p-NF-κB Expression, Inflammatory Cytokine Production, and Pathological Changes in EAE Mice—To investigate the effect of A20 on the development of EAE, we constructed lentiviral expression vectors with GFP of LV-A20 shRNA (including LV-ctrl shRNA) and injected them into the mice through the tail vein. Seven days later, EAE was induced by MOG(35–55) for 16 days. Clinical scores showed that LV-A20 shRNA-infected mice developed severe EAE, including the advancement of the onset of EAE (Fig. 9*G*). Meanwhile, the EAE mice injected with LV-A20 shRNA showed a significantly down-regulated A20 protein level and an enhanced NF-κB activation in the brain, compared with LV-ctrl shRNA-infected mice. However, the NF-κB expression showed no statistical significance among different groups (Fig. 9, *A* and *B*). The levels of IL-6, TNF-α, MIP-2, and MCP-1/5 were all remarkably elevated in LV-A20 shRNA-infected mice compared with LV-ctrl shRNA-infected mice (Fig. 9*C*). Furthermore, the EAE mice pretreated with LV-A20 shRNA had more inflammatory cell infiltration (Fig. 9*D*) and more severe demyelination lesion in the spinal cord (Fig. 9, *E* and *F*). Similar changes in the brain were also observed (data not shown). Collectively, these findings reveal that silencing the A20 expression markedly aggravates tissue lesions both in brains and spinal cords of EAE mice, which may be associated with an increased inflammatory reaction via the A20/NF-κB pathway.

DISCUSSION

Reportedly, miRNA regulation may play an important role in the development or prevention of some autoimmune diseases (30). Here, we demonstrated that miR-873 was co-up-regulated both in EAE mice and in astrocytes. Upon IL-17 stimulation, miR-873 can directly target the A20 gene and promote NF-κB activation, leading to the enhanced production of inflammatory and chemotactic cytokines both *in vivo* and *in vitro*. More importantly, inhibiting endogenous miR-873 *in vivo* greatly decreased inflammation and demyelination, thereby ameliorating the development of EAE.

IL-17 can contribute to EAE pathogenesis; specifically, the blockade of IL-17 signaling in mouse astrocytes attenuates EAE (9). As one of the resident cells in the CNS, astrocytes serve as a bridge between the CNS and the immune system (10). Aberrant expression of cytokines and chemokines in astrocytes often accompanies CNS disorders, such as MS, Alzheimer disease, and brain injury/trauma (10, 31). Our data showed that the levels of IL-17, IL-6, TNF-α, MIP-2, and MCP-1/5 were increased rapidly on day 20 in the EAE model. Meanwhile, A20 or p-NF-κB/p65 expression either decreased or increased by 20 days after the EAE induction, respectively. Additionally, the levels of several of the above cytokines in primary astrocytes upon IL-17 stimulation significantly increased at 6 h, whereas A20 protein expression decreased, and p-NF-κB/p65 level increased remarkably. However, it remains unclear how IL-17 regulates inflammatory cytokine production of mouse astrocytes and the EAE pathological process.

In a recent study, Zhu *et al.* (32) demonstrated that IL-17 contributed to autoimmune pathogenesis by suppressing miR-23b expression in radio-resident cells and promoting proinflammatory cytokine synthesis. Moreover, strong evidence suggests that miRNAs play an important role in a wide range of complex human diseases by targeting multiple transcripts (33, 34). During the past few years, studies of miRNA expression profiles from blood cells and CNS lesions of MS patients have demonstrated that aberrant miRNA levels and functions are associated with MS (26, 35–37). However, the changes in miRNA expression profiles both in the brain tissue of EAE mice and in mouse astrocytes stimulated with IL-17 have not yet been revealed. Thus, by employing miRNA microarray and real-time PCR, we surveyed the differentially expressed miRNAs *in vivo* and *in vitro*. Notably, there were 11 miRNAs that differentially co-up-regulated both in the of EAE mice and in the astrocytes stimulated with IL-17 for 3 h. It is clear that different miRNA may suppress the same target gene expression. Hence, we screened and identified some up-regulated miRNAs complementary to A20 3′-UTR. The results of the luciferase assay and Western blot suggest that miR-873 (a co-up-regulated miRNA *in vivo* and *in vitro*) can directly target A20 mRNA and markedly modulate A20 protein expression.

Recently, several studies confirmed that miR-326, miR-155, miR-182, and miR-146a affect the functions of T and B cells, thereby modulating autoimmune diseases (28, 29, 38, 39). Furthermore, the microRNA-132/212 cluster affects Th17 differentiation and EAE pathogenesis (40, 41). After exposure to

FIGURE 9. **The effects of A20 gene knockdown on p-NF-κB expression and pathological changes in the brain or spinal cord of EAE mice.** Mice were injected with recombinant LV-A20 shRNA or LV-ctrl shRNA lentivirus for 7 days and then immunized with MOG(35–55) for 16 days ($n = 10$ mice/group). *A*, the EAE mice treated with LV-A20 shRNA lentivirus showed a marked down-regulation of A20 protein in the brain tissue using Western blot analysis ($n = 3$). *B*, Western blot analysis showed that LV-A20 shRNA lentivirus-infected mice presented a notable up-regulation of p-NF-κB/p65 protein in the brain tissue compared with other groups. *C*, the levels of IL-6, TNF-α, MIP-2, and MCP-1/5 in the brain tissue and in peripheral blood of LV-A20 shRNA lentivirus-infected mice and LV-ctrl shRNA lentivirus-infected mice were analyzed using real-time PCR and ELISA, respectively. *D*, H&E staining showed more inflammatory infiltration in the spinal cords of EAE mice pretreated with LV-A20 shRNA lentivirus (*scale bars*, 50 μm). *E*, demyelination lesions in the white matter of the spinal cords isolated from different treatment mice were analyzed with LFB staining (*scale bars*, 50 μm). *F*, under EM, the EAE mice in the LV-A20 shRNA-infected group exhibited a clearer loosening and disruption of the myelin sheath of the spinal cord (*scale bars*, 1 μm). *G*, the clinical scores for EAE mice infected with LV-A20 shRNA or LV-ctrl shRNA lentivirus ($n = 10$ mice/group). *, $p < 0.05$; **, $p < 0.01$ *versus* NC groups. #, $p < 0.05$; ##, $p < 0.01$ *versus* LV-ctrl shRNA groups. *Error bars*, S.E.

interferon-γ (IFN-γ) and lipopolysaccharide (LPS) *in vitro*, the expressions of miRNA-155, miRNA-146a, and miRNA-146b were up-regulated in mouse astrocytes (42). In the current study, we found that miR-873 was significantly up-regulated in primary mouse astrocytes upon IL-17 stimulation and that the overexpression of miR-873 in astrocytes not only enhanced the levels of inflammatory cytokines and chemokines, such as IL-6, TNF-α, MIP-2, and MCP-1/5, including p-NF-κB/p65, but also reduced A20 protein expression in response to IL-17 stimulation. In contrast, the knockdown of miR-873 with LNA-anti-miR-873 in mouse astrocytes effectively reversed these changes.

It was revealed that A20-deficient mice died prematurely as a result of spontaneous multiorgan inflammation and cachexia (43). The mice lacking A20 specifically in the myeloid compartment (Tnfaip3$^{fl/fl}$LysM-Cre) also developed autoimmune disease, and Tnfaip3$^{fl/fl}$LysM-Cre mice exhibited elevated serum levels of inflammatory cytokines (*e.g.* TNF, IL-1β, and IL-6) that were also mirrored in joint tissue (44). It was initially found that multiple NF-κB-activating stimuli could induce A20 expression via NF-κB binding sites in the A20 promoter (45), and subsequent studies also found that the overexpression of A20 inhibited NF-κB activation in response to different stimuli (46). Thus, A20 is an important negative feedback regulator of NF-κB that is essential for immune homeostasis (47). Our current study also demonstrated that silencing A20 enhanced the phosphorylation of NF-κB and strongly drove the production of inflammatory cytokines and chemokines (IL-6, TNF-α, MIP-2, and MCP-1/5) in the astrocytes upon IL-17 stimulation. In addition, the administration of PDTC markedly diminished the increased level of these cytokines and the p-NF-κB/p65 protein in mouse astrocytes at 6 h after IL-17 treatment (Fig. 6, *D–F*). Taken together, our findings indicate that the co-up-regulated miR-873 *in vivo* and *in vitro* promotes the production of inflammatory cytokines and chemokines via inhibiting A20 and enhancing the NF-κB activation.

It has been reported that the blockade of IL-17 signaling in mouse astrocytes could attenuate the damage of EAE mice (9). Given that the inhibition of miR-873 *in vitro* could increase A20 expression and decrease NF-κB activation and inflammatory cytokine production, we constructed the lentiviral expression vectors of LV-miR-873 and LV-miR-873 sponge and injected them into the EAE mice to further corroborate our results *in vitro*. The data *in vivo* showed that the overexpression of miR-873 suppressed A20 protein expression and facilitated the phosphorylation of NF-κB as well as the production of IL-6, TNF-α, MIP-2, and MCP-1/5 in EAE mice. Correspondingly, the inhibition of endogenous miR-873 *in vivo* greatly decreased the inflammation and demyelination of the CNS and ameliorated the development of EAE. In addition, silencing the A20 gene markedly aggravated tissue lesions both in the brain and spinal cord of EAE mice. Here it is worth mentioning that although injection of LV-miR-873 *in vivo* might impact the function of other cells besides astrocytes, knockdown of endogenous miR-873 greatly decreased the pathologic changes in CNS of mouse with EAE, indicating that the effect is partially mediated by decreasing production of proinflammatory cytokines in mouse astrocytes at least.

In summary, our study presents evidence suggesting that IL-17 induces aberrant expression of miRNA in brain astrocytes, and the co-expression miRNA (miR-873), both in the brain tissue of EAE mice and in mouse primary brain astrocytes upon stimulation with IL-17, can regulate the production of inflammatory cytokines and chemokines *in vitro* and *in vivo*, resulting in effects on the development of EAE. Thus, these findings provide new insights into the role of miRNA and a novel therapeutic target for the corresponding autoimmune disease.

Acknowledgments—We thank Professor Xufeng Huang (University of Wollongong, Australia), Professor Feng Lin (Cleveland Clinic), and Professor Kuiyang Zheng (Xuzhou Medical College, China) for reviewing the manuscript.

REFERENCES

1. Creeke, P. I., and Farrell, R. A. (2013) Clinical testing for neutralizing antibodies to interferon-β in multiple sclerosis. *Ther. Adv. Neurol. Disord.* **6,** 3–17
2. Hauser, S. L., and Oksenberg, J. R. (2006) The neurobiology of multiple sclerosis: genes, inflammation, and neurodegeneration. *Neuron* **52,** 61–76
3. Bettelli, E., Oukka, M., and Kuchroo, V. K. (2007) T(H)-17 cells in the circle of immunity and autoimmunity. *Nat. Immunol.* **8,** 345–350
4. Korn, T., Bettelli, E., Oukka, M., and Kuchroo, V. K. (2009) IL-17 and Th17 Cells. *Annu. Rev. Immunol.* **27,** 485–517
5. Marwaha, A. K., Leung, N. J., McMurchy, A. N., and Levings, M. K. (2012) TH17 cells in autoimmunity and immunodeficiency: protective or pathogenic? *Front. Immunol.* **3,** 129
6. Kebir, H., Kreymborg, K., Ifergan, I., Dodelet-Devillers, A., Cayrol, R., Bernard, M., Giuliani, F., Arbour, N., Becher, B., and Prat, A. (2007) Human TH17 lymphocytes promote blood-brain barrier disruption and central nervous system inflammation. *Nat. Med.* **13,** 1173–1175
7. Zepp, J., Wu, L., and Li, X. (2011) IL-17 receptor signaling and T helper 17-mediated autoimmune demyelinating disease. *Trends Immunol.* **32,** 232–239
8. Hemdan, N. Y., Birkenmeier, G., Wichmann, G., Abu El-Saad, A. M., Krieger, T., Conrad, K., and Sack, U. (2010) Interleukin-17-producing T helper cells in autoimmunity. *Autoimmun. Rev.* **9,** 785–792
9. Kang, Z., Altuntas, C. Z., Gulen, M. F., Liu, C., Giltiay, N., Qin, H., Liu, L., Qian, W., Ransohoff, R. M., Bergmann, C., Stohlman, S., Tuohy, V. K., and Li, X. (2010) Astrocyte-restricted ablation of interleukin-17-induced Act1-mediated signaling ameliorates autoimmune encephalomyelitis. *Immunity* **32,** 414–425
10. Allen, N. J., and Barres, B. A. (2009) Neuroscience: glia: more than just brain glue. *Nature* **457,** 675–677
11. Wilson, E. H., Weninger, W., and Hunter, C. A. (2010) Trafficking of immune cells in the central nervous system. *J. Clin. Invest.* **120,** 1368–1379
12. Meares, G. P., Ma, X., Qin, H., and Benveniste, E. N. (2012) Regulation of CCL20 expression in astrocytes by IL-6 and IL-17. *Glia* **60,** 771–781
13. Junker, A., Hohlfeld, R., and Meinl, E. (2011) The emerging role of microRNAs in multiple sclerosis. *Nat. Rev. Neurol.* **7,** 56–59
14. Thamilarasan, M., Koczan, D., Hecker, M., Paap, B., and Zettl, U. K. (2012) MicroRNAs in multiple sclerosis and experimental autoimmune encephalomyelitis. *Autoimmun. Rev.* **11,** 174–179
15. Waschbisch, A., Atiya, M., Linker, R. A., Potapov, S., Schwab, S., and Derfuss, T. (2011) Glatiramer acetate treatment normalizes deregulated microRNA expression in relapsing remitting multiple sclerosis. *PloS One* **6,** e24604
16. Lescher, J., Paap, F., Schultz, V., Redenbach, L., Scheidt, U., Rosewich, H., Nessler, S., Fuchs, E., Gärtner, J., Brück, W., and Junker, A. (2012) MicroRNA regulation in experimental autoimmune encephalomyelitis in mice and marmosets resembles regulation in human multiple sclerosis

lesions. *J. Neuroimmunol.* **246,** 27–33
17. Wertz, I. E., O'Rourke, K. M., Zhou, H., Eby, M., Aravind, L., Seshagiri, S., Wu, P., Wiesmann, C., Baker, R., Boone, D. L., Ma, A., Koonin, E. V., and Dixit, V. M. (2004) De-ubiquitination and ubiquitin ligase domains of A20 downregulate NF-κB signalling. *Nature* **430,** 694–699
18. Hymowitz, S. G., and Wertz, I. E. (2010) A20: from ubiquitin editing to tumour suppression. *Nat. Rev. Cancer* **10,** 332–341
19. Brambilla, R., Persaud, T., Hu, X., Karmally, S., Shestopalov, V. I., Dvoriantchikova, G., Ivanov, D., Nathanson, L., Barnum, S. R., and Bethea, J. R. (2009) Transgenic inhibition of astroglial NF-κB improves functional outcome in experimental autoimmune encephalomyelitis by suppressing chronic central nervous system inflammation. *J. Immunol.* **182,** 2628–2640
20. Musone, S. L., Taylor, K. E., Nititham, J., Chu, C., Poon, A., Liao, W., Lam, E. T., Ma, A., Kwok, P. Y., and Criswell, L. A. (2011) Sequencing of TNFAIP3 and association of variants with multiple autoimmune diseases. *Genes Immun.* **12,** 176–182
21. Qian, Y., Liu, C., Hartupee, J., Altuntas, C. Z., Gulen, M. F., Jane-Wit, D., Xiao, J., Lu, Y., Giltiay, N., Liu, J., Kordula, T., Zhang, Q. W., Vallance, B., Swaidani, S., Aronica, M., Tuohy, V. K., Hamilton, T., and Li, X. (2007) The adaptor Act1 is required for interleukin 17-dependent signaling associated with autoimmune and inflammatory disease. *Nat. Immunol.* **8,** 247–256
22. Qin, H., Niyongere, S. A., Lee, S. J., Baker, B. J., and Benveniste, E. N. (2008) Expression and functional significance of SOCS-1 and SOCS-3 in astrocytes. *J. Immunol.* **181,** 3167–3176
23. Liu, X. M., Pei, D. S., Guan, Q. H., Sun, Y. F., Wang, X. T., Zhang, Q. X., and Zhang, G. Y. (2006) Neuroprotection of Tat-GluR6–9c against neuronal death induced by kainate in rat hippocampus via nuclear and non-nuclear pathways. *J. Biol. Chem.* **281,** 17432–17445
24. Liu, L., Qiu, W., Wang, H., Li, Y., Zhou, J., Xia, M., Shan, K., Pang, R., Zhou, Y., Zhao, D., and Wang, Y. (2012) Sublytic C5b-9 complexes induce apoptosis of glomerular mesangial cells in rats with Thy-1 nephritis through role of interferon regulatory factor-1-dependent caspase 8 activation. *J. Biol. Chem.* **287,** 16410–16423
25. Goverman, J. (2009) Autoimmune T cell responses in the central nervous system. *Nat. Rev. Immunol.* **9,** 393–407
26. Guerau-de-Arellano, M., Smith, K. M., Godlewski, J., Liu, Y., Winger, R., Lawler, S. E., Whitacre, C. C., Racke, M. K., and Lovett-Racke, A. E. (2011) Micro-RNA dysregulation in multiple sclerosis favours pro-inflammatory T-cell-mediated autoimmunity. *Brain* **134,** 3578–3589
27. Murugaiyan, G., Beynon, V., Mittal, A., Joller, N., and Weiner, H. L. (2011) Silencing microRNA-155 ameliorates experimental autoimmune encephalomyelitis. *J. Immunol.* **187,** 2213–2221
28. Du, C., Liu, C., Kang, J., Zhao, G., Ye, Z., Huang, S., Li, Z., Wu, Z., and Pei, G. (2009) MicroRNA miR-326 regulates TH-17 differentiation and is associated with the pathogenesis of multiple sclerosis. *Nat. Immunol.* **10,** 1252–1259
29. O'Connell, R. M., Kahn, D., Gibson, W. S., Round, J. L., Scholz, R. L., Chaudhuri, A. A., Kahn, M. E., Rao, D. S., and Baltimore, D. (2010) MicroRNA-155 promotes autoimmune inflammation by enhancing inflammatory T cell development. *Immunity* **33,** 607–619
30. Iborra, M., Bernuzzi, F., Invernizzi, P., and Danese, S. (2012) MicroRNAs in autoimmunity and inflammatory bowel disease: crucial regulators in immune response. *Autoimmun. Rev.* **11,** 305–314
31. Dong, Y., and Benveniste, E. N. (2001) Immune function of astrocytes. *Glia* **36,** 180–190
32. Zhu, S., Pan, W., Song, X., Liu, Y., Shao, X., Tang, Y., Liang, D., He, D., Wang, H., Liu, W., Shi, Y., Harley, J. B., Shen, N., and Qian, Y. (2012) The microRNA miR-23b suppresses IL-17-associated autoimmune inflammation by targeting TAB2, TAB3 and IKK-α. *Nat. Med.* **18,** 1077–1086
33. Garofalo, M., and Croce, C. M. (2011) microRNAs: Master regulators as potential therapeutics in cancer. *Annu. Rev. Pharmacol. Toxicol.* **51,** 25–43
34. Nagpal, J. K., Rani, R., Trink, B., and Saini, K. S. (2010) Targeting miRNAs for drug discovery: a new paradigm. *Curr. Mol. Med.* **10,** 503–510
35. Fenoglio, C., Ridolfi, E., Galimberti, D., and Scarpini, E. (2012) MicroRNAs as active players in the pathogenesis of multiple sclerosis. *Int. J. Mol. Sci.* **13,** 13227–13239
36. Jr Ode, F., Moore, C. S., Kennedy, T. E., Antel, J. P., Bar-Or, A., and Dhaunchak, A. S. (2012) MicroRNA dysregulation in multiple sclerosis. *Front. Genet.* **3,** 311
37. Martinelli-Boneschi, F., Fenoglio, C., Brambilla, P., Sorosina, M., Giacalone, G., Esposito, F., Serpente, M., Cantoni, C., Ridolfi, E., Rodegher, M., Moiola, L., Colombo, B., De Riz, M., Martinelli, V., Scarpini, E., Comi, G., and Galimberti, D. (2012) MicroRNA and mRNA expression profile screening in multiple sclerosis patients to unravel novel pathogenic steps and identify potential biomarkers. *Neurosci. Lett.* **508,** 4–8
38. Stittrich, A. B., Haftmann, C., Sgouroudis, E., Kühl, A. A., Hegazy, A. N., Panse, I., Riedel, R., Flossdorf, M., Dong, J., Fuhrmann, F., Heinz, G. A., Fang, Z., Li, N., Bissels, U., Hatam, F., Jahn, A., Hammoud, B., Matz, M., Schulze, F. M., Baumgrass, R., Bosio, A., Mollenkopf, H. J., Grün, J., Thiel, A., Chen, W., Höfer, T., Loddenkemper, C., Löhning, M., Chang, H. D., Rajewsky, N., Radbruch, A., and Mashreghi, M. F. (2010) The microRNA miR-182 is induced by IL-2 and promotes clonal expansion of activated helper T lymphocytes. *Nat. Immunol.* **11,** 1057–1062
39. Lu, L. F., Boldin, M. P., Chaudhry, A., Lin, L. L., Taganov, K. D., Hanada, T., Yoshimura, A., Baltimore, D., and Rudensky, A. Y. (2010) Function of miR-146a in controlling Treg cell-mediated regulation of Th1 responses. *Cell* **142,** 914–929
40. Nakahama, T., Hanieh, H., Nguyen, N. T., Chinen, I., Ripley, B., Millrine, D., Lee, S., Nyati, K. K., Dubey, P. K., Chowdhury, K., Kawahara, Y., and Kishimoto, T. (2013) Aryl hydrocarbon receptor-mediated induction of the microRNA-132/212 cluster promotes interleukin-17-producing T-helper cell differentiation. *Proc. Natl. Acad. Sci. U.S.A.* **110,** 11964–11969
41. Hanieh, H., and Alzahrani, A. (2013) MicroRNA-132 suppresses autoimmune encephalomyelitis by inducing cholinergic anti-inflammation: a new Ahr-based exploration. *Eur. J. Immunol.* **43,** 2771–2782
42. Mor, E., Cabilly, Y., Goldshmit, Y., Zalts, H., Modai, S., Edry, L., Elroy-Stein, O., and Shomron, N. (2011) Species-specific microRNA roles elucidated following astrocyte activation. *Nucleic Acids Res.* **39,** 3710–3723
43. Lee, E. G., Boone, D. L., Chai, S., Libby, S. L., Chien, M., Lodolce, J. P., and Ma, A. (2000) Failure to regulate TNF-induced NF-κB and cell death responses in A20-deficient mice. *Science* **289,** 2350–2354
44. Matmati, M., Jacques, P., Maelfait, J., Verheugen, E., Kool, M., Sze, M., Geboes, L., Louagie, E., Mc Guire, C., Vereecke, L., Chu, Y., Boon, L., Staelens, S., Matthys, P., Lambrecht, B. N., Schmidt-Supprian, M., Pasparakis, M., Elewaut, D., Beyaert, R., and van Loo, G. (2011) A20 (TNFAIP3) deficiency in myeloid cells triggers erosive polyarthritis resembling rheumatoid arthritis. *Nat. Genet.* **43,** 908–912
45. Krikos, A., Laherty, C. D., and Dixit, V. M. (1992) Transcriptional activation of the tumor necrosis factor α-inducible zinc finger protein, A20, is mediated by κB elements. *J. Biol. Chem.* **267,** 17971–17976
46. Song, H. Y., Rothe, M., and Goeddel, D. V. (1996) The tumor necrosis factor-inducible zinc finger protein A20 interacts with TRAF1/TRAF2 and inhibits NF-κB activation. *Proc. Natl. Acad. Sci. U.S.A.* **93,** 6721–6725
47. Shembade, N., and Harhaj, E. W. (2012) Regulation of NF-κB signaling by the A20 deubiquitinase. *Cell. Mol. Immunol.* **9,** 123–130